Title Page

Title:

Different tree-ring width sensitivities to satellite-based soil moisture from dry, moderate and wet pedunculate oak (*Quercus robur* L.) stands across a southeastern distribution margin

Author block:

Saša Kostić, Wolfgang Wagner, Saša Orlović, Tom Levanič, Tzvetan Zlatanov, Ernest Goršić, Lazar Kesić, Bratislav Matović, Nickolay Tsvetanov, Dejan B. Stojanović

- **Saša Kostić**, Institute of Lowland Forestry and Environment, University of Novi Sad, Antona Čehova 13d, 21000 Novi Sad, Serbia. e-mail: sasa.kostic@uns.ac.rs
  ORCID ID: 0000-0003-4111-8534
- **Wolfgang Wagner,** TU Wien, Department of Geodesy and Geoinformation, Vienna, Austria. e-mail: wolfgang.wagner@geo.tuwien.ac.at
  ORCID ID: 0000-0001-7704-6857
- **Saša Orlović**, Institute of Lowland Forestry and Environment, University of Novi Sad, Antona Čehova 13d, 21000 Novi Sad, Serbia. e-mail: sasao@uns.ac.rs
  ORCID ID: 0000-0002-2724-1862
- **Tom Levanič**, Slovenian Forestry Institute, Večna pot 2, 1000 Ljubljana, Slovenia. e-mail: tom.levanic@gozdis.si
  ORCID ID: 0000-0002-0986-8311
- **Tzvetan Zlatanov,** Institute of Biodiversity and Ecosystem Research, Bulgarian Academy of Sciences, 2 Gagarin Street, 1113 Sofia, Bulgaria. e-mail: tmzlatanov@gmail.com
  ORCID ID: 0000-0003-4205-3429

- **Ernest Goršić,** Faculty of Forestry, Department of Forest Management Planning and Inventory, University of Zagreb, 10002 Zagreb, Croatia. e-mail: egorsic@sumfak.hr
  ORCID ID: 0000-0002-5775-9232
- **Lazar Kesić,** Institute of Lowland Forestry and Environment, University of Novi Sad, Antona Čehova 13d, 21000 Novi Sad, Serbia. e-mail: kesic.lazar@uns.ac.rs
  ORCID ID: 0000-0003-2643-9727
- **Bratislav Matović**, Institute of Lowland Forestry and Environment, University of Novi Sad, Antona Čehova 13d, 21000 Novi Sad, Serbia. e-mail: bratislav.matovic@uns.ac.rs
  ORCID ID: 0000-0002-4664-6355
- **Nickolay Tsvetanov,** University of Forestry - Sofia, 10 Kliment Ohridski Blvd., 1797 Sofia, Bulgaria. e-mail: nicktsvetanov@ltu.bg
  ORCID ID: 0000-0002-3156-4939
- **Dejan B. Stojanović (corresponding author)**, Institute of Lowland Forestry and Environment, University of Novi Sad, Antona Čehova 13d, 21000 Novi Sad, Serbia. e-mail: dejan.stojanovic@uns.ac.rs
  ORCID ID: 0000-0003-2967-2049

Abstract:

Associations of pedunculate oak (*Quercus robur* L.) radial growth with satellite-based soil moisture (SM) during the intensive tree growth period over a 30-year time span (1980–2010) were analyzed. This study included tree-ring width (TRW) chronologies from 22 stands located in four southeastern (SE) European countries (Slovenia, Croatia, Serbia and Bulgaria), which were grouped into three wetness groups (WGs): dry (<650 mm), moderate (650-750 mm), and wet (>750 mm), following the annual sum of precipitation. High correlation strengths during the intensive growth period—late spring and early summer months (April to June) was noted, which was opposite to the trend in late summer months. Variations in detrended TRW (TRWi) sensitivity to SM were also observed among the WGs. Specifically, the TRWi chronologies from the dry and wet WGs provided a greater number of significant correlations (p<0.01) than trees from the moderate WG did. In wetter stands, TRWi correlated more negatively in the wettest (spring) months, while the correlation was weaker in summer months; these trends were opposite to those of trees growing in drier conditions, that had the strongest responses to SM. A generalized additive mixed model (GAMM) based on 38 variables indicated that the fit for SM and radial growth was as strong as the fits for other traditionally measured parameters (temperature, precipitation, and river water level) and calculated drought indices (standardized precipitation index and the Ellenberg index) and TRW. Additionally, radial growth chronologies from drier sites had stronger fits with surrounding environmental factors. In conclusion, our findings suggest that SM can potentially be used as a reliable remote sensing indicator of the soil wetness in oak forests, which affects tree productivity and radial growth patterns and provides a new opportunity in dendrochronology research on larger scales.

Keywords: Soil moisture; Radial growth; Remote sensing; Dendrochronology; Oak.

1. Introduction

Forest ecosystems in southeastern (SE) Europe will be exposed to a warmer and likely drier climate in the near future, following the 4.5 and more severe representative concentration pathway (RCP) scenarios (IPCC, 2019). In 21st century, extreme drought events have increased in Europe (Spinoni et al., 2018). These new stand conditions will adversely affect forests, compromising both wood quality and radial growth (Boisvenue and Running, 2006; Paquette et al., 2018). According to the RCP scenarios, the most severe impacts are expected on climate-sensitive species such as pedunculate oak (*Quercus robur* L.), resulting in significantly reduced radial growth until 2100 (Bauwe et al., 2018). This prediction is of great importance because pedunculate oak is the most important economic species in lowland forests in SE Europe; furthermore, it is one of the most endangered tree species in temperate forest ecosystems (EUFORGEN, 2009; Hanewinkel et al., 2012).

Pedunculate oak sensitivity to water loss is complex issue. Oak forests from the analyzed SE European region showed that they are highly sensitive to temperature and precipitation variations (Skiadaresis et al., 2019; Kostić et al., 2019) as well as drought events (Arvai et al., 2018; Losseau et al., 2020). Intensive oak declines were observed in 2011-12 (Stojanović et al., 2015a; Losseau et al. 2020) and especially after drought event occurred 2018-19 (Scharnweber et al., 2020), which was based on oxygen ($\delta^{18}O$) and carbon ($\delta^{13}C$) stable isotopes past climate reconstruction is labeled as one of the two driest years in last two millennia (Büntgen et al., 2021). Hence, their chronologies are recognized as one of the most suitable proxy records of past hydroclimatic conditions (Büntgen et al., 2011, 2021; Nechita et al., 2012). In dendroecological studies focusing on pedunculate oak, water availability has been recognized as one of the most important climate-related factors contributing to radial increment reduction. For example, Stojanović et al. (2015a) reported a significant radial increment reduction in a lowland forest from northern Serbia during periods of very low water levels in the Danube River, while Kostić et al. (2021) revealed that above- and under-ground water sources equally affect oak radial growth. Likewise, significant relationships between annual precipitation and tree-ring width (TRW), as well as calculated meteorological drought indices, such as the standardized precipitation index (SPI), standardized precipitation evapotranspiration index (SPEI), Palmer drought severity index (PDSI), and many others were confirmed (e.g., Stojanović et al., 2018; Heklau et al., 2019; Losseau et al., 2020; Kostić et al., 2021).

Remote sensing satellites have provided a growing number of new data sets describing vegetation cover and other Earth surface features (Wang et al., 2004). This has resulted in an increased use of remotely sensed data in dendrochronology (Southworth et al., 2013; Reiche et al., 2016; White et al., 2016). Up to now, only few remotely sensed indices were used in dendrochronology. The normalized difference vegetation index (NDVI) is one of the mostly used indices, while indices such as new primary production (NPP) and soil moisture (SM) have just recently been introduced. In particular, NDVI datasets are widely used, as the NDVI allows the estimation of forest cover degradation based on canopy color changes (Carlson and Ripley, 1997). Recent studies indicate that the NDVI is highly correlated with radial increments in different environments (Srur et al., 2011; Brehaut and Danby, 2018; Correa-Díaz et al., 2019; Muñoz et al., 2014; Martínez-Fernández et al., 2019). Likewise, NPP showed a significant but lower correlation with radial growth in dry conditions than NDVI (Southworth et al., 2020). The remotely sensed index used in this study was soil moisture (SM), which was derived from microwave remote sensing measurements (see Wagner et al. 2007 for more information). Serving as a potential proxy for water availability in forest ecosystems (Kim et al., 2020), microwave-based SM data significantly differ from NDVI data in terms of their prognostic value; such data depict changes in trees via tree crown reflectance. Hence, SM should be a valuable and uniform water proxy for the whole Earth system from 1978 to date, with wide implications in water-plant related studies.

1.1. Aim

Although the radial increment is one of the most important indicators of forest productivity, its relationship with water availability in forest ecosystems remained insufficiently studied. Fortunately, SM can currently be measured from different sources, either *in situ* sensors, satellite-based measurements (Babaeian et al., 2019) or modeled values (Cianfrani et al., 2019). Even though the relations between the different data sources are not fully understood, it is clear that all sources are particularly useful for tracking changes in SM over time (Brocca et al., 2017)

The main objective of this research was to examine pedunculate oak radial increment sensitivity to satellite-based SM from different wetness conditions across their populations distributed throughout SE Europe. Differences between tree sensitivity to SM across stands characterized by water availability, deficit and/or surplus provide new insights into the potential of using SM as an ecological indicator of soil water content and its impact on oak forest productivity (interpreted as the radial increment). In line with the main objective of this study, we defined the following research hypotheses:

(1) Wetness conditions significantly affect the radial growth dynamics.
(2) Radial growth is strongly correlated with satellite-based SM.
(3) The radial growth response to SM varies according to stand wetness conditions.

2. Material and methods

2.1. Analyzed region and stand characteristics

The present study was conducted on 22 stands across four SE European countries. The sample consisted of 341 individual TRW series. Specifically, we had three locations in Slovenia (SLO; 67 TRW series; SLO_1, 2 and 3), two in Croatia (CRO; 35 TRW series; CRO_1 and 2), 14 in Serbia (SRB; 171 TRW series, SRB_1 to 13) and four in Bulgaria (BGR; 65 TRW series; BGR_1 to 4), as shown in Table 1 and Fig. 1.

In the analyzed region, pedunculate oak grows in different site conditions. To represent this diversity, this study utilized tree ring data from representative ecologically different stands. The dataset used included flood lowland oak forests at less than 100 m a.s.l. from the Danube and Sava River basins, as well as oak forests from elevations up to 400 m a.s.l. The highest and lowest elevations were recorded for Sorško polje (SLO_1, 388 m a.s.l.) and Stara vratična (SRB_12 and SRB_13, 78 m a.s.l.), respectively. Similarly, the longitude ranged from 14.422989° (Sorško polje, SLO_1) to 26.571423° (Gorna topchiya, BGR_4), whereas the latitude ranged from 46.490978° (Murka šuma, SLO_3) to 42.178805° (Dolna topchiya, BGR_3).

The meteorological data were extracted from the E-OBS gridded database (version 23.1e from March 2021; Copernicus: European Union's Earth observation programme). In the analyses, we used annual mean temperatures (in °C, TEMP) and annual sums of precipitation (in mm, PCPT). Based on gridded data, differences in TEMP and PCPT were noted among the analyzed stands. The TEMP ranged from 12.45°C (Dolna topchiya, BGR_3) to 14.47°C (Tulovska koriya, BGR_1), while the PCPT ranged from 58.68 mm (Gorna topchiya, BGR_4) to 82.46 mm (Smogava, SRB_10 and SRB_11). Based on the PCPT values, TRW chronologies were classified into three wetness groups – WGs (dry: <650 mm; moderate: 650-750 mm; and wet: >750 mm PCPT).

2.2. Tree-ring width collections and satellite-based SM observations

All remotely sensed data were extracted from the ESA Climate Change Initiative (CCI) SM dataset (http://www.esa-soilmoisture-cci.org/) version 0.4.4; see Gruber et al. (2019) for details. The ESA CCI SM data are derived by fusing individual satellite SM data sets from a series of passive and active microwave missions, as laid out by Wagner et al. (2013). The data are expressed in volumetric units [m^3 m^{-3}] and come as daily files sampled to a 0.25° (~27-28 km) worldwide grid. In this study, data from 1979 to 2010 were used. This microwave-based SM dataset essentially reflects changes in the dielectric properties of the soil caused by different SM levels (Dorigo et al., 2017).

For this study, we collected published and unpublished TRW chronologies from SE Europe (see Table 1.). The sample included only visually healthy, mature, dominant trees from natural stands. Each individual TRW series was calculated as an average from two core samples and was interpreted as the whole annual radial increment (early and late wood together).

2.3. Data processing

All statistical data processing was carried out using R (R Core Team, 2013). The map with the analyzed stands was produced with the "Raster" R package using SRTM data (Jarvis et al., 2008). The results were interpreted for each tree, stand, and WG (according to the annual PCPT of the stands, see Table 1).

The TRW chronologies were single detrended using the “dplR” package (Bunn, 2008). In this study, we used a detrending method commonly used in dendrochronology, which consists of a modified detrending method with a negative exponential curve described by Equation 1: $f(t) = aexp(bt) + k$, according to Fritts (2001). In this paper, we used measured TRW and detrended TRW (TRWi) chronologies, with smoothed lines with confidence intervals for $p<0.05$. The smoothed curves were obtained with the generalized additive model (GAM) in the R package "ggplot2". The bootstrapped Pearson's correlations between TRWi and SM were calculated for the period 1980-2010 using the R package "treeclim" (Zang and Biondi, 2015). The used bootstrap Pearson’s correlation equation is:

Eq. 1.

$$r_{boot} = \frac{\sum xy - nn\underline{xy}}{\sqrt{[(\sum x^2 - nx'^2)(\sum y^2 - ny'^2)]}}$$

where r_{boot} is the bootstrap Pearson's correlation coefficient, n is the sample size and x and y are correlated variables.

Tree grouping into WGs based on detrended radial growth and its sensitivity to SM was performed via principal component analysis (PCA), based on 1980–2010 period. Statistically significant differences were tested using one-way analyzes of variance for $p < 0.05$. Grouping was performed via ANOVA honestly significant difference (HSD) Tukey post-hoc test.

2.3.1. The generalized additive mixed model (GAMM) processing

Following the increasing application of nonlinear models in radial growth modeling (Marchand et al., 2020; Kostić et al., 2021; Wernicke et al., 2021) and after testing both linear and non-linear model approaches, we selected a non-linear model for this study. Using a generalized additive mixed model (GAMM), we described the relationships among the radial growth chronologies and surrounding factors from different WGs. In detail, 38 variables were used for the GAMM construction, with equal effects on the model. The GAMM outputs were used to describe the implications and reliability of the interactions of the remotely sensed SM of the radial growth-surrounded environment and compare the remotely sensed data with traditionally measured parameters such as temperature, precipitation, river water level, etc.

A GAMMs were provided by Eq. 2, and a GAMMs were then constructed for each WG (dry, moderate, and wet), each for a 30-year timespan (1980–2010). In all three cases, the same 38 variables were used as the inputs to the second model. Only TRW chronologies that covered the mentioned 30-year period were included in the model. In total, 118, 152, and 71 tree TRW chronologies from dry, moderate, and wet stands were included in the second model. The GAMMs were developed using the "mgcv" R package (Wood, 2015) via Equation 2:

Eq. 2.

$$
\begin{aligned}
TRWi \sim 1 &+ s(PRCP) + s(PRCP_{MAM}) + s(PRCP_{JJA}) + s(PRCP_{Y2}) + s(TEMP) + s(TEMP_{MAM}) \\
&+ s(TEMP_{JJA}) + s(TEMP_{Y2}) + s(SM) + s(SM_{MAM}) + s(SM_{JJA}) + s(SM_{Y2}) + s(RWL) \\
&+ s(RWL_{MAM}) + s(RWL_{JJA}) + s(SPI\ 3_{MAR}) + s(SPI\ 3_{JUNE}) + s(SPI\ 3_{AUG}) + s(SPI\ 6_{MAR}) \\
&+ s(SPI\ 6_{JUNE}) + s(SPI\ 6_{AUG}) + s(SPI\ 12_{MAR}) + s(SPI\ 12_{JUNE}) + s(SPI\ 12_{AUG}) \\
&+ s(SPI\ 24_{MAR}) + s(SPI\ 24_{JUNE}) + s(SPI\ 24_{AUG}) + s(SPI\ 36_{MAR}) + s(SPI\ 36_{JUNE}) \\
&+ s(SPI\ 36_{AUG}) + s(SPI\ 48_{MAR}) + s(SPI\ 48_{JUNE}) + s(SPI\ 48_{AUG}) + s(SPI\ 60_{MAR}) \\
&+ s(SPI\ 60_{JUNE}) + s(SPI\ 60_{AUG}) + \left(\frac{Site}{Tree}\right) + CorCAR1\left(Year \mid \left(\frac{Site}{Tree}\right)\right)
\end{aligned}
$$

where TRWi denotes the detrended radial growth. Temperature, precipitation, and river water level were interpreted for annual and two-year-long periods, based on the vegetation period from the previous (or two years prior) September to August following the year, and for two three-month-long periods. The first three months covered spring months and an intensive tree growth period (March to May), and the next months included summer months from June to August (the most unfavorable period for tree growth). Drought was interpreted from the standardized precipitation index (SPI; see Vicente-Serrano et al., 2010). The SPI was calculated from three representative and key months for radial increment during the vegetation period (March, June, and August) for 3-, 6-, 12-, 24-, 36-, 48-, and 60-months accumulation periods. In total, 21 SPIs were calculated and included in the GAMM. The abbreviations and descriptions of all 38 used variables and the sources of the precipitation, temperature, and river water level measurements and the calculated or remotely sensed wetness indices are listed in Appendix A. In the GAMM, the $\left(\frac{Site}{Tree}\right)$ is used as a random effect.

We used a CorCAR1 as autocorrelation function in the GAMM. The smoother in mgcv :: gamm was defined using the generalized cross validation (GCV) technique. Following Wood (2017), the GAMM results were interpreted via the Adj. R^2 (adjusted coefficient of determination), the EDF (estimated degree of freedom) and F (F-test with statistical significance level *p*). The models were validated using K' (smoother's maximal potential values) and k-index with a *p* significance level (test of sufficient number of basis function, respected the GAMM residual pattern, see Wood (2007) for more details). The GAMM performance was also checked visually on the basis of its residuals deviation.

For the GAMM, we used a commonly used significance code, where (^{NS}) indicated nonsignificant, $p > 0.05$. Asterisks denote the significance level, where (*), (**), and (***) indicate that the model fitting was significant at $p < 0.05$, < 0.01, and < 0.001, respectively.

3. Results

3.1. Radial growth chronologies from dry, moderate and wet stands

Trend of radial growth across pedunculate oak southeastern populations in different wetness conditions was analyzed using a TRW series from 341 trees for the timespan from 1685 to 2018. In 333 years long timespan, radial growth variations were shaped via stand wetness conditions. In the TRW chronologies taken from the dry, moderate, and wet WGs, significant variations were observed (Fig. 2), but the highest and lowest growth was observed in the same periods. Due to significantly lower number of TRW series, the first part (before 1850s) should be considered with caution and in further interpretation we will focused on the second part of analyzed chronologies. When comparing the TRWi chronologies for the three WGs, we found that oaks that grew in more extreme conditions (dry and wet stands) deviated more strongly than oaks from the moderate WG. Likewise, higher one year decreasing peaks were detected in oaks from wet WG, compared to other two WGs.

In unfavorable and drought periods in the 21st century, only oaks from the moderate WG had an increasing trend, while oaks from the driest stand had constantly decreasing trend. Trees from the wet WG varied to a greater extent over time. In some cases, these variations could be linked with drought. For example, after extreme drought periods across Europe in the 2000s, 2011-12, and 2017-18, oaks from wet stands had a stronger decreasing trend (but a faster recovery) than trees from the dry WGs, which were constantly decreasing but at a significantly slower rate, starting in the 1990s.

3.2. Radial growth sensitivity to SM

The sensitivity of radial growth to SM was investigated by bootstrapped Pearson correlation analysis of satellite-based SM data and detrended radial growth (TRWi) chronologies. The correlation strength between SM and TRWi for each analyzed tree on a monthly level during the 1979−2010 period is presented in Fig. 3, which shows that the TRWi sensitivity to SM tended to increase during the intensive vegetation period (spring and early summer) of tree-ring formation.

Likewise, the SM−TRWi correlation strength varied among WGs. As shown in Fig. 3, radial increments noted in the dry (PRCP < 650 mm) and moderate (PRCP 650–750 mm) WGs exhibited positive responses to SM, opposite to those from wetter stands (PRCP > 750 mm). As a result, trees from the dry and moderate WGs benefited the most from the increase in SM in summer months, which are the driest and hottest months in the temperate climate zone.

On the other hand, trees from the wet and dry WGs were adversely affected by SM during the wettest months in a vegetation period (i.e., April and May). SM had the strongest negative impact on trees growing in sites that were in the wet WG. During the spring months, which are the wettest in the vegetation period, tree radial growth from the wet WG provided a negative response to SM, opposite of the responses of trees growing in moderately wet and dry stands. Thus, based on the TRWi chronologies (Fig. 2) and the lowest TRWi sensitivity to SM, oaks from the moderate WG showed the best performance in light of intensive climate change as less water/drought/ sensitive specimens.

As shown in Fig. 4, 55−75% of SM−TRWi correlations were statistically significant ($p < 0.05$), which were separated in three group based on HSD Tukey ANOVA post-hoc test for the same statistically significance. February and April strongly deviated from the other months. It is worth noting that the highest number of statistically significant correlations were obtained for April, followed by June and May, while much lower numbers were recorded for September and August. Hence, overall, the lowest SM−TRWi correlation strength values were recorded during the early spring and late summer months, while SM in September had important influence on radial growth performances.

3.3. WG associations with radial growth and its sensitivity to SM

Satellite-based SM data should be interpreted as a measure of soil water availability at analyzed sites. In accordance with this statement based on pedunculate oak data, SM should be a valuable proxy of radial increment variations. The results yielded by the present study indicated that the classification of analyzed sites into three WGs based on the total annual precipitation corresponded well to the differences in radial increment sensitivity to SM. Following non-linear TRWi distributs, we chose the GAMM to describe the associations of TRWi with SM and calibrated the SM influence related to traditionally measured factors.

Additionally, the spatial arrangement of trees assigned to different WGs was obtained through PCA. The PCA revealed similarities in spatial differentiation between TRWi (Fig. 5-a) and TRWi sensitivity to SM (Fig. 5-b). As shown in Fig. 5-a, trees belonging to the moderate WG exhibited the smallest intrapopulation variability, whereas those from the moderate and wet WGs were relatively similar.

The GAMMs (Eq. 2.) were used to compare the SM possibilities in radial growth GAMM modelling with other commonly used key meteorological factors such as temperature, precipitation, drought indices and underground wetness modifiers such as river water level (Table 2). The GAMM in all three cases (dry, moderate, and wet WGs) produced a moderately strong fitting. The adjusted coefficients of determinations (Adj. R^2) were 0.57, 0.459, and 0.436 for the dry, moderate, and wet WGs, respectively. Out of the 38 variables that were included in the GAMM construction, more than ~2/3 were statistically significant at $p<.05$ (dry: 11/38; moderate: 8/38; wet: 14/38) on the basis of the F-test significance level. Only in two cases (SPI 36_{AUG} and SPI 48_{MAR}) was statistical significance not observed for any of the three GAMMs. The K-index was ≥0.87, and the K values were 9 for all variables.

The precipitation, temperature, river water level, SM, EQ, and SPI indices exerted different influences on the TRWi GAMM models. In almost all of the three spring months (March-May), the average temperature, precipitation, river water level, and SM more strongly affected radial growth than they did in the summer months (June-August). The observed pattern consisted of an intensive growth phase during spring months in the temperate climate zone. The SPI indices, encompassing 21 variables, did not present as a clear pattern as the abovementioned parameters did, following 3- to 60-month-long accumulation periods.

Soil moisture variables (SM, SM_{Y2}, SM_{MAM}, and SM_{JJA}) produced correlations that were as strong as those for the other traditionally measured parameters (temperature, precipitation, and river water level) and affected the TRWi in the constructed GAMMs (Eq. 2). This indicates that remotely sensed SM is a reliable environmental factor for radial growth modeling, equally as traditionally measured parameters.

Based on the GAMM approach (Eq. 2.), oaks growing in drier conditions are more sensitive to surrounding stand factors than oaks growing in moderate and wet stand conditions. The strongest fitting was noted for oaks in the dry WG (Adj. R^2=0.57), while the lowest Adj R^2 was noted for the wet WG (0.436). Equal deviations in GAMM (Eq. 2.) residuals were noted for all three WGs (Fig 6). Only in a few years, e.g., 1982 and 2001 for the moderate WG and 1984 for the wet WG, were stronger deviations noted. The GAMM that included oaks from the dry WG had the smallest deviations (Fig 6-a).

4. Discussion

4.1. Pedunculate oak radial growth sensitivity across SE Europe

Pedunculate oak radial growth sensitivity and performances were intensively research in last decades (see Haneca et al., 2009 and Sochová et al., 2021 review papers). Likewise, oaks were recognized as a key species to past-climate, -drought, and -hydrology reconstructions in Europe, due to their strong radial growth, and C and O stable isotope responses to surrounding environment, especially to water deviations (Büntgen et al., 2011, 2021). Likewise, pedunculate oak is one of the most valuable forest tree species in SE Europe (Oprea et al., 2018), and as such, it has been the focus of many studies investigating tree ring sensitivity to changing environmental conditions. In published papers, researchers have mainly focused on TRW measurements as whole- or early- and late-wood radial increments separately (Nechita et al., 2012; 2019; Stojanović et al., 2015a; 2018; Arvai et al., 2018; Kostić et al., 2021, etc.). Although informative (Levanič et al., 2011; Urban et al., 2020), other tree ring properties (such as wood anatomy, density, and C, H, and O stable isotopes) have rarely been measured in oaks from the analyzed region, but widely used on European scale (e.g. Büntgen et al., 2011; 2021). Nonetheless, a few studies from SE Europe analyzed carbon stable isotopes (Levanič et al., 2011; Kostić et al., 2019) and wood anatomy (Jevšenak et al., 2019) and (as expected) revealed significant sensitivity to the surrounding environmental factors.

Across its distribution range, pedunculate oak was recognized as a highly sensitive species to intensive climate change (Nechita et al., 2012; Bauwe et al., 2018), as well as to water availability deviations, meteorological conditions, drought (Stojanović et al., 2018), soil properties (Kostić et al., 2021), and underground wetness (Skiadaresis et al., 2019). The sample examined in the present study included stands from areas characterized by diverse climate conditions. The variations in radial growth noted in this study could be attributed to different stand conditions, which is in accordance with recent findings about oak radial increment plasticity to the surrounding environmental stressors (Arvai et al., 2018; Stojanović et al., 2018; Skiadaresis et al., 2019; Jevšenak et al., 2019; etc.).

Furthermore, following different scenarios of forest productivity, a decreasing trend was recorded in the first two decades of the 21st century, and it has been projected to continue in the future (Bauwe et al., 2018). Assisted migration and climate-smart forest management should be one of the adaptation tools to new climate conditions (del Castillo et al., 2019; Williamson et al., 2019). Wood quality and annual radial increment dynamics are important traits which could be considered during oak forest management because pedunculate oak is one of the most expensive wood types from SE European forests (Glavonjic et al., 2005; Attocchi, 2015). Thus, our comparative research of TRW chronologies and the obtained variations provide insight into their wood productivity under different stand wetness conditions, which would be of interest to forest practitioners and stake holders during decision making process.

4.2. The TRW–SM relation and its plasticity to the stand water availability

The use of remotely sensed indices in dendrochronology is still in an early stage. At present, the most commonly used remote sensing index is the NDVI, which is based on near-infrared color changes in tree canopies. As this variable is directly related to photosynthesis intensity and tree performance and health conditions, it can be reflected in radial increments (Brehaut and Danby, 2018). On the other hand, the used SM parameter measured soil drought, which except water limited a nutrient uptake via root and provide imbalance in metabolism which also limited radial increment (Taiz et al., 2015).

Soil water availability to plants is defined by many environmental and climate factors, which reflected on oak radial increment (Kostić et al., 2021). For example, soil characteristics (structure and organic matter) define the dynamics of water absorption (from atmosphere and underground water sources) and its availability to plants (Asgarzadeh et al., 2010). Furthermore, most environmental pollutants (heavy metals, salt, fuel, etc.) limit water with macro- and microelements absorption into the plant, which detrimentally affect plant metabolism and their growth (Wu et al., 2010; Taiz et al., 2015). However, some root characteristics, such as root architecture, which defines the depth of the active root zone, have been shown to affect water absorption in field experiments (Manske et al., 2002) and could perhaps be replicated to plant sensitivity to satellite-based environmental indices, such as SM.

Our results indicated significant correlations between SM and TRW, with notable variations among months, locations, and site conditions. These findings are in line with those yielded by other regional dendroecological studies of pedunculate oak radial increment sensitivity to stand conditions. Stojanović et al. (2015a), for example, reported a relationship between groundwater level in lowland oak forests and TRW, while Netsvetov et al. (2017) noted PCPT and TEMP impacts on radial increment reduction. Some drought indices based on meteorological measurements, such as SPI, SPEI, and RDI, have also been investigated before, and the results indicate high pedunculate oak TRW sensitivity (Stojanović et al., 2018, Losseau et al., 2020).

Several authors that have examined the sensitivity of pedunculated oak QURO TRW to stand conditions noted prolonged effects of environmentally induced stress on radial increment reduction (Stojanović et al., 2018, Zheng et al., 2019). Our SM vs. TRWi associations support this specific finding. Following their correlations on a monthly level, prolonged effects were not observed, which was the opposite result of the one-, two-year averages (see the GAMM outputs). The absence of meaningful correlations during winter months might be attributed to erroneous remotely sensed SM measurements when the soil is frozen or covered by snow (Dorigo et al., 2017). Hence, microwave-based SM data can be more readily used during vegetation seasons in northern climates or during whole years in climates without snowy and icy periods.

Pedunculate oak is a highly drought-sensitive species (Nechita et al., 2012; Árvai et al., 2018). In the present study, deviations and decreasing trends in water availability significantly reduced radial increments of pedunculate oak specimens (Skiadaresis et al., 2019). This result is in line with the statement that marginal populations are more climate sensitive than when they are in optimal stand conditions in most boreal tree species, such as silver fir, beech, and analyzed oak (Askeyev et al., 2005; Guo et al., 2014; Stjepanović et al., 2018). Newer studies on pedunculate oak TRW indicate higher variation and a significant decreasing trend in radial increment in 21st century (Árvai et al., 2018; Bauwe et al., 2018). These strong variations among years were marked in recent research on stable carbon isotope ratio, which can be used to reconstruct plant stress conditions during the analyzed tree-ring chronologies (Levanič et al., 2011; Kostić et al., 2019).

4.3. Remotely sensed SM as a reliable ecological indicator of oak forest productivity?

Pedunculate oak radial growth is highly sensitive to SM. The sensitivity of radial increment to soil water availability (derived from SM) differed considerably across the analyzed stands, whereby stands classified in the wet and dry WGs more often expressed a significant correlation between SM and radial increment. In wet stands, SM was more weakly correlated in the wettest (spring) months and less strongly correlated in the summer months. However, trees growing under dry conditions showed the strongest response to SM. Similarly, strong correlations were found during the intensive growth period in contrast to the early spring and late summer months. Furthermore, pedunculate oaks from the moderate and wet WGs were less sensitive to SM, which set them apart as suitable for the new upcoming changes in the surrounding stand conditions. In addition, we observed a prolonged effect (up to 4 years) of SM on radial growth, which must be included in further implications of SM in dendrochronological studies based on radial growth. Likewise, the constructed GAMM showed that the fitting for SM and radial growth was as strong as the fittings for other traditionally measured parameters and radial growth.

Finally, our research provides a new insight into the implications of remotely sensed parameters such as SM in tree-ring research. In particular, the revealed correlation strengths and between-stand and WG variations open new opportunities for further research into pedunculate oak and other temperate woody species sensitivity to water availability. Additionally, a broad introduction of remote sensing in forestry could enable much faster collection of valuable environmental data in a short and continuous time frame and contribute to a deeper understanding of forest ecosystems and radial growth dynamics.

Acknowledgements

SK and **DS** acknowledge the financial support from the Science Fund of the Republic of Serbia, Program for excellent projects of young researchers (PROMIS) via project "Understanding *Quercus robur* L. vitality loss using stable carbon isotopes ratio ($\delta^{13}C$), drought and remotely sensed indices and development of strategies for adaptation to changing climate conditions (TreeVita)" and from the Ministry of Education, Science and Technological Development of the Republic of Serbia (No. 451-03-68/2020-14/ 200197).

TL acknowledge the financial support from the Slovenian Research Agency - research core funding No. P4-0107 Program research group "Forest Biology, Ecology and Technology" at the Slovenian Forestry Institute and basic research project J4-8216 "Mortality of lowland oak forests - consequence of lowering underground water or climate change?"

DS acknowledge the research grant at TU Wien through JESH programme funded by Austrian Academy of Sciences in 2018. **DS** acknowledge the useful discussion and support from Prof. Wouter Arnoud Dorigo (Department of Geodesy and Geoinformation TU Wien).

EG acknowledge the financial support from Zagreb University through Support programme for scientific and art activities funded by Croatian Ministry of Science and Education.

TZ acknowledge the financial support from the Bulgarian National Science Fund (BNSF) via project No. DCOST 01/7/19.10.2018.

Authors' contributions

SK, WW and DS conceived the ideas and designed the experiment. SK wrote the manuscript. TL, EG, TZ, BM, NT, LK, DS and NT contributed to data collection. All authors contributed critically to the drafts and gave final approval for publication.

Conflict of interest: none declared.

Appendix A

Table A1. Abbreviations, descriptions, and sources of the GAMM variables.

No.	Abbreviation	Variable	Description	Source
1	PRCP	Annual sum of precipitation	Units: mm m^{-2}, frequency: daily measurements.	E-OBS, 23.1e version (Copernicus: European Union's Earth observation programme)
2	$PRCP_{MAM}$	March-May sum od precipitation		
3	$PRCP_{JJA}$	June-August sum of precipitation		
4	$PRCP_{Y2}$	Two-year sum of precipitation		
5	TEMP	Anual temperature	Units: °C, frequency: daily measurements.	
6	$TEMP_{MAM}$	March-May average temperature		
7	$TEMP_{JJA}$	June-August average temperature		
8	$TEMP_{Y2}$	Two your average temperature		
9	SM	Soil moisture	Soil moisture (m^3 m^{-3}), Satellite taken, in first ~10 cm soil depth, at 0.25° (~27-28 km) resolution. The combined daily observation system from the ESA soil moisture dataset (see Dorigo et al., 2017 for more information).	European space agency climate change initiative
10	SM_{MAM}	March-May soil mosture		
11	SM_{JJA}	June-August soil moisture		
12	SM_{Y2}	Two-year soil moisture		
13	RWL	Annual river water level	River water level (cm), based on daily observations.	Hydrometheorological services of Republic of Serbia; National Institute of Meteorology and Hydrology (Bulgaria); National Hydrometeorological Institute (Croatia); Hydrometeorological Institute of Slovenia (Slovenia)
14	RWL_{MAM}	March-May river water level		
15	RWL_{JJA}	June-August river water level		
15	SPI	Standard precipitation index	Calculated from daily TEMP data from E-OBS data base.	

References

Askeyev, O.V., Tischin, D., Sparks, T.H., et al., 2005. The effect of climate on the phenology, acorn crop and radial increment of pedunculate oak (*Quercus robur*) in the middle Volga region, Tatarstan, Russia. Int. J. Biometeorol. 49, 262–266. https://doi.org/10.1007/s00484-004-0233-3

Arvai, M., Morgos, A., Kern, Z., 2018. Growth-climate relations and the enhancement of drought signals in pedunculate oak (*Quercus robur* L.) tree-ring chronology in Eastern Hungary. iForest 11(2), 267. https://doi.org/10.3832/ifor2348-011

Asgarzadeh, H., Mosaddeghi, M.R., Mahboubi, A.A., Nosrati, A., Dexter, A.R., 2010. Soil water availability for plants as quantified by conventional available water, least limiting water range and integral water capacity. Plant. Soil. 335(1-2), 229–244. https://doi.org/10.1007/s11104-010-0410-6

Attocchi, G., 2015. Silviculture of oak for high-quality wood production. Diss. (sammanfattning/summary) Alnarp: Sveriges lantbruksuniv., Acta Universitatis Agriculturae Sueciae.

Bauwe, A., Jurasinski, G., Scharnweber, T., Schroeder, C., Lennartz, B., 2015. Impact of climate change on tree-ring growth of Scots pine, common beech and pedunculate oak in northeastern Germany. iForest 9, 1–11. https://doi.org/10.3832/ifor1421-008

Boisvenue, C., Running, S.W., 2006. Impacts of climate change on natural forest productivity– evidence since the middle of the 20^{th} century. Global Change Biol. 12(5), 862–882. https://doi.org/10.1111/j.1365-2486.2006.01134.x

Brehaut, L., Danby, R.K., 2018. Inconsistent relationships between annual tree ring-widths and satellite-measured NDVI in a mountainous subarctic environment. Ecol. Indic. 91, 698–711. https://doi.org/10.1016/j.ecolind.2018.04.052

Brocca, L., Ciabatta, L., Massari, C., Camici, S., Tarpanelli, A., 2017. Soil moisture for hydrological applications: open questions and new opportunities. Water 9(2), 140.

Bunn, A.G., 2008. A dendrochronology program library in R (dplR). Dendrochronologia 26(2), 115–124. https://doi.org/10.1016/j.dendro.2008.01.002

Büntgen, U., Tegel, W., Nicolussi, K., McCormick, M., et al., 2011. 2500 years of European climate variability and human susceptibility. Science, 331(6017), https://doi.org/578–582. 10.1126/science.1197175

Büntgen, U., Urban, O., Krusic, P. J., Rybníček, M., et al., 2021. Recent European drought extremes beyond Common Era background variability. Nat. Geosci., 14(4), 190-196. https://doi.org/10.1038/s41561-021-00698-0

Carlson, T.N., Ripley, D.A., 1997. On the relation between NDVI, fractional vegetation cover, and leaf area index. Remote Sens. Environ. 62(3), 241–252. https://doi.org/10.1016/S0034-4257(97)00104-1

Coolen-Maturi, T., Elsayigh, A., 2010. A comparison of correlation coefficients via a three-step bootstrap approach. J. Math. Res. 2(2), 3–10. https://doi.org/10.5539/jmr.v2n2p3

Correa-Díaz, A., Silva, L.C.R., Horwath, W.R., Gómez-Guerrero, A. et al., 2019. Linking remote sensing and dendrochronology to quantify climate-induced shifts in high-elevation forests over space and time. J. Geophys. Res. Biogeosci. 124(1), 166–183. https://doi.org/10.1029/2018JG004687

Cianfrani, C., Buri, A., Vittoz, P., Grand, S., Zingg, B., Verrecchia, E., Guisan, A., 2019. Spatial modelling of soil water holding capacity improves models of plant distributions in mountain landscapes. Plant Soil 438(1-2), 57–70. https://doi.org/10.1007/s11104-019-04016-x

del Castillo, E.M., Longares, L.A., Serrano-Notivoli, R., Sass-Klaassen, U.G., de Luis, M., 2019. Spatial patterns of climate–growth relationships across species distribution as a forest management tool in Moncayo Natural Park (Spain). Eur. J. For. Res. 138(2), 299–312. https://doi.org/10.1007/s10342-019-01169-3

Dorigo, W., Wagner, W., Albergel, C., Albrecht, F. et al., 2017. ESA CCI Soil Moisture for improved Earth system understanding: State-of-the art and future directions. Remote Sens. Environ. 203, 185–215. https://doi.org/10.1016/j.rse.2017.07.001

EUFORGEN, 2009, Distribution map of Pedunculate oak (*Quercus robur*) EUFORGEN 2009. [Available at: http://www.euforgen.org/]

Fritts HC., 2001. Tree rings and climate. Blackburn Press, Caldwell.

Glavonjic, B., Jovic, D., Kankaras, R., Vasiljevic, A., 2005. Forest and forest products country profile: Serbia and Montenegro. UN.

Guo, Q., 2014. Central-marginal population dynamics in species invasions. Front. Ecol. Evol. 2, 23. https://doi.org/10.3389/fevo.2014.00023

Gruber, A., Scanlon, T., van der Schalie, R., Wagner, W., Dorigo, W., 2019. Evolution of the ESA CCI Soil Moisture climate data records and their underlying merging methodology. Earth Syst. Sci. Data 1–37. https://doi.org/10.5194/essd-11-717-2019

Haneca, K., Čufar, K., Beeckman, H., 2009. Oaks, tree-rings and wooden cultural heritage: a review of the main characteristics and applications of oak dendrochronology in Europe. J. Archaeol. Sci. 36(1), 1-11. https://doi.org/10.1016/j.jas.2008.07.005

Hanewinkel, M., Cullmann, D. A., Schelhaas, M.-J., Nabuurs, G.-J., Zimmermann, N.E., 2012. Climate change may cause severe loss in the economic value of European forest land. Nat. Clim. Change 3(3), 203–207. https://doi.org/10.1038/nclimate1687

Heklau, H., Jetschke, G., Bruelheide, H., Seidler, G., Haider, S., 2019. Species-specific responses of wood growth to flooding and climate in floodplain forests in Central Germany. iForest. 12(3), 226–236. https://doi.org/10.3832/ifor2845-012

Hogg, E.H., Barr, A.G., Black, T.A., 2013. A simple soil moisture index for representing multi-year drought impacts on aspen productivity in the western Canadian interior. Agr. Forest Meteorol. 178, 173–182. https://doi.org/10.1016/j.agrformet.2013.04.025

IPCC (Intergovernmental Panel on Climate Change), (2019. Climate change and land. An IPCC Special Report on climate change, desertification, land degradation, sustainable land management, food security, and greenhouse gas fluxes in terrestrial ecosystems. Summary for Policymakers. Jarvis, A., Reuter, H.I., Nelson, A., Guevara, E., 2008. Hole-filled seamless SRTM data V4, International Centre for Tropical Agriculture (CIAT). [Available at: http://srtm.csi.cgiar.org]

Jevšenak, J., Goršić, E., Stojanović, D.B., Matović, B., Levanič, T., 2019. Sapwood characteristics of *Quercus robur* species from the south-western part of the Pannonian Basin. Dendrochronologia 54, 64–70. https://doi.org/10.1016/j.dendro.2019.02.006

Kostić, S., Levanič, T., Orlović, S., Matović, B., Stojanović, D.B., 2019. Penduncturate and Turkey oaks radial increment and stable carbon isotope response to climate conditions through time. *Poplar* 204, 29–35.

Kostić, S., Kesić, L., Matović, B., Orlović, S., Stojnić, S., Stojanović, D.B., 2021. Soil properties are significant modifiers of pedunculate oak (*Quercus robur* L.) radial increment variations and their sensitivity to drought. *Dendrochronologia*, 67, 125838. https://doi.org/10.1016/j.dendro.2021.125838

Kim, H., Wigneron, J. P., Kumar, S., Dong, J., Wagner, W., et al., 2020. Global scale error assessments of soil moisture estimates from microwave-based active and passive satellites and land surface models over forest and mixed irrigated/dryland agriculture regions. Remote Sens. Environ., 251, 112052.

Losseau, J., Jonard, M., Vincke, C., 2020. Pedunculate oak decline in southern Belgium: a long-term process highlighting the complex interplay among drought, winter frost, biotic attacks, and masting. Can. J. For. Res. 50(4), 380–389. https://doi.org/10.1139/cjfr-2019-0341

Levanič, T., Čater, M., McDowell, N.G., 2011. Associations between growth, wood anatomy, carbon isotope discrimination and mortality in a *Quercus robur* forest. *Tree Physiol*. 31(3), 298–308. https://doi.org/10.1093/treephys/tpq111

Marchand, W., Girardin, M. P., Hartmann, H., Depardieu, C., Isabel, N., Gauthier, S., Boucher, E., Bergeron, Y. 2020. Strong overestimation of water-use efficiency responses to rising CO2 in tree-ring studies. *Glob Chan Biol*, 26(8), 4538–4558. https://doi.org/10.1111/gcb.15166

Manske, G.G., Vlek, P.L., 2002. Root architecture–wheat as a model plant. Plant roots: The hidden half, 3, 249–259. https://doi.org/10.1201/9780203909423.ch15

Martínez-Fernández, J., Almendra-Martín, L., de Luis, M., González-Zamora, A., Herrero-Jiménez, C., 2019. Tracking tree growth through satellite soil moisture monitoring: A case study of *Pinus halepensis* in Spain. Remote Sens. Environ. 235, 111422. https://doi.org/10.1016/j.rse.2019.111422

Muñoz, A.A., Barichivich, J., Christie, D.A., Dorigo, W., Sauchyn, D., González-Reyes, Á., Villalba, R., Lara, A., Riquelme, N. and González, M.E., 2014. Patterns and drivers of Araucaria growth. Austral. Ecology 39, 158–169. https://doi.org/10.1111/aec.12054

Nechita, C., Macovei, I., Popa, I., Badea, O.N., Apostol, E.N., Eggertsson, Ó., 2019. Radial growth-based assessment of sites effects on pedunculate and greyish oak in southern Romania. Sci. Total Environ. 694, 133709. https://doi.org/10.1016/j.scitotenv.2019.133709

Nechita, C., Popa I., 2012. The relationship between climate and radial growth for the oak (*Quercus robur* L.) in the western plain of Romania. Carpathian J. Earth Environ. Sci. 7(3), 137–144.

Netsvetov, M., Sergeyev, M., Nikulina, V., Korniyenko, V., Prokopuk, Y., 2017. The climate to growth relationships of pedunculate oak in steppe. Dendrochronologia 44, 31–38. https://doi.org/10.1016/j.dendro.2017.03.004

Oprea, A.M., Borlea, G.F., Dronca, D., 2018. Oak species–providing renewable and sustainable raw materials, enriching the ecosystems services and fulfilling the social demands. Case-study–western Romania. Scientific Papers. Series E. Land Reclamation, Earth Observation & Surveying, Environmental Engineering 7, 225–233.

Paquette, A., Vayreda, J., Coll, L., Messier, C., Retana, J., 2018. Climate change could negate positive tree diversity effects on forest productivity: a study across five climate types in Spain and Canada. *Ecosystems* 21(5), 960–970. https://doi.org/10.1007/s10021-017-0196-y

R Core Team, 2013. R: A language and environment for statistical computing. Vienna, Austria.

Reiche, J., Lucas, R., Mitchell, A.L., Verbesselt, J. et al., 2016. Combining satellite data for better tropical forest monitoring. Nat. Clim. Change 6(2), 120–122. https://doi.org/10.1038/nclimate2919

Scharnweber, T., Smiljanic, M., Cruz-García, R., Manthey, M., Wilmking, M., 2020. Tree growth at the end of the 21st century-the extreme years 2018/19 as template for future growth conditions. Environ. Res. Lett., 15(7), 074022. https://doi.org/10.1088/1748-9326/ab865d

Sochová, I., Kolář, T., Rybníček, M., 2021. A Review of oak dendrochronology in Eastern Europe. Tree-Ring Res. 77(1), 10-19.

Skiadaresis, G., Schwarz, J.A., Bauhus, J., 2019. Groundwater extraction in floodplain forests reduces radial growth and increases summer drought sensitivity of pedunculate oak trees (*Quercus robur* L.). Front. For. Glob. Change 2, 5. https://doi.org/10.3389/ffgc.2019.00005

Southworth J, Rigg L, Gibbes C, Waylen P, Zhu L, McCarragher S, Cassidy L., 2013. Integrating Dendrochronology, Climate and Satellite Remote Sensing to Better Understand Savanna Landscape Dynamics in the Okavango Delta, Botswana. Land. 2013; 2(4):637-655. https://doi.org/10.3390/land2040637

Spinoni, J., Vogt, J. V., Naumann, G., Barbosa, P., Dosio, A., 2018. Will drought events become more frequent and severe in Europe?. Int J Climatol, 38(4), 1718-1736. https://doi.org/10.1002/joc.5291

Srur, A. M., Villalba, R., Baldi, G., 2011. Variations in *Anarthrophyllum rigidum* radial growth, NDVI and ecosystem productivity in the Patagonian shrubby steppes. Plant Ecol. 212(11), 1841. https://doi.org/10.1007/s11258-011-9955-6

Stjepanović, S., Matović, B., Stojanović, D., Lalić, B., Levanič, T., Orlović, S., Gutalj, M., 2018. The Impact of Adverse Weather and Climate on the Width of European Beech (*Fagus sylvatica* L.) Tree Rings in Southeastern Europe. Atmosphere 9(11), 451. https://doi.org/10.3390/atmos9110451

Stojanović, D.B., Levanič, T., Matović, B., Orlović, S., 2015a. Growth decrease and mortality of oak floodplain forests as a response to change of water regime and climate. Eur. J. For. Res. 134(3), 555–567. https://doi.org/10.1007/s10342-015-0871-5

Stojanović, D., Levanič, T., Matović, B., Bravo-Oviedo, A., 2015b. Climate change impact on a mixed lowland oak stand in Serbia. Annals of Silvicultural Research 39(2), 94–99. http://dx.doi.org/10.12899/asr-1126

Stojanović, D., Levanič, T., Matović, B., Stjepanović, S., Orlović, S., 2018. Growth response of different tree species (oaks, beech and pine) from SE Europe to precipitation over time. Dendrobiology 79, 97–110. http://dx.doi.org/10.12657/denbio.079.009

Taiz, L., Zeiger, E., Møller, I. M., Murphy, A., 2015. Plant physiology and development (No. Ed. 6). Sinauer Associates Incorporated.

Urban, O., Ač, A., Kolář, T., Rybníček, M., Pernicová, et al., 2020. The dendroclimatic value of oak stable isotopes. Dendrochronologia, 125804. https://doi.org/10.1016/j.dendro.2020.125804

Vicente-Serrano, S. M., Beguería, S., López-Moreno, J. I., 2010. A multiscalar drought index sensitive to global warming: the standardized precipitation evapotranspiration index. J. Clim. 23(7), 1696–1718. https://doi.org/10.1175/2009JCLI2909.1

Zang, C., Biondi, F., 2015. Treeclim: an R package for the numerical calibration of proxy-climate relationships. Ecography 38(4), 431–436. https://doi.org/10.1111/ecog.01335

Zheng, W., Gou, X., Su, J., Fan, H., Yu, A., Liu, W., Deng, Y., Manzanedo, R.D., Fonti, P., 2019. Physiological and growth responses to increasing drought of an endangered tree species in Southwest China. Forests 10, 514. https://doi.org/10.3390/f10060514

Wagner, W., Blöschl, G., Pampaloni, P., Calvet, J.C., Bizzarri, B., Wigneron, J.P., Kerr, Y., 2007. Operational readiness of microwave remote sensing of soil moisture for hydrologic applications. Hydrology Research 38(1), 1–20.

Wagner, W., Hahn, S., Kidd, R., Melzer, T., et al., 2013. The ASCAT soil moisture product: A review of its specifications, validation results, and emerging applications. Meteorol. Z. 22(1), 5–33. https://doi.org/10.1127/0941-2948/2013/0399

Wang, J., Rich, P.M., Price, K.P., Kettle, W.D., 2004. Relations between NDVI and tree productivity in the central Great Plains. Int. J. Remote Sens. 25(16), 3127–3138. https://doi.org/10.1080/0143116032000160499

White, J.C., Coops, N.C., Wulder, M.A., Vastaranta, M., Hilker, T., Tompalski, P., 2016. Remote sensing technologies for enhancing forest inventories: A review. Can. J. Remote Sens. 42(5), 619–641. https://doi.org/10.1080/07038992.2016.1207484

Wernicke, J., Körner, M., Möller, R., Seltmann, C.T., Jetschke, G., Martens, S., 2020. The potential of generalized additive modelling for the prediction of radial growth of Norway spruce from Central Germany. *Dendrochronologia*, 63, 125743.

Williamson, T.B., Johnston, M.H., Nelson, H.W., Edwards, J.E., 2019. Adapting to climate change in Canadian forest management: Past, present and future. For. Chron. 95(2), 76–90. https://doi.org/10.5558/tfc2019-015

Wood, S., Wood, M.S., 2015. Package ‘mgcv’. R package version, 1, 29.

Wood, S.N., 2017. Generalized additive models: an introduction with R. CRC press.

Wu, C., Spongberg, A.L., Witter, J.D., Fang, M., Czajkowski, K.P., 2010. Uptake of pharmaceutical and personal care products by soybean plants from soils applied with biosolids and irrigated with contaminated water. Environ. Sci. Technol. 44(16), 6157–6161. https://doi.org/10.1021/es1011115

Table legend

Table 1. Analyzed stand locations and meteorological and site characteristics.

Table 2. Generalized additive mixed model (GAMM) outputs to oaks that growing on drier, moderate, and wetter stands.

Figure legend

Figure 1. Map of the study area.

Figure 2. TRWi chronologies of oaks that growth on (a) dry, (b) moderate, (c) wet stands, and (d) sample depth.

Figure 3. TRW-SM correlation strength distributions on a monthly level.

Note: Box-plots outliers are set to $p < .01$. Box are interquartile range, and horizontal line is median value. Time span: 1980 to 2010.

Figure 4. Monthly percentage of statistically significant correlations, with error bars and HSD Tukey post hoc test, for 95% significance

Figure 5. PCA of (a) TRW data and (b) TRWi vs, SM correlation strength, in timespan from 1979 to 2010, with wetness groups as grouping variable.

Figure 6. GAMM residuals for oak that growing in dry (a), moderate (b), and wet (c) wetness group. In timespan from 1980 to 2010.

Table 1. Analyzed stand locations and meteorological and site characteristics.

Country	Location	Wetness group	TRW chronology	Tree No.	Longitude	Latitude	Altitude (m a.s.l.)	PCPT* (mm/m^2)	TEMP* (°C)	Reference
Slovenia	Sorško polje	Dry	SLO_1	16	14.422989	46.232964	388	638.3	13.92	Unpublished data
	Krakovski pragozd	Moderate	SLO_2	29	15.406855	45.876006	165	731.1	14.27	Unpublished data
	Murska Šuma	Moderate	SLO_3	22	16.528080	46.490978	157	655.9	14.02	Unpublished data
Croatia	Lipovljani	Moderate	CRO_1	16	16.816667	45.366667	105	656.9	14.12	Unpublished data
	Spačva	Dry	CRO_2	19	18.816667	45.100000	92	644.0	13.99	Unpublished data
Serbia	Bački Monoštor	Dry	SRB_1	10	19.007222	45.832417	84	643.8	14.1	Unpublished data
		Dry	SRB_2	10	19.007222	45.832417	84	643.3	13.99	Unpublished data
	Kragujevac	Dry	SRB_3	18	21.095540	44.142830	91	643.2	13.94	Unpublished data
	Blate	Moderate	SRB_4	20	19.138056	45.004167	87	731.8	14.46	Unpublished data
		Wet	SRB_5	20	19.213889	44.955556	86	766.0	14.36	Stojanović et al., 2015a
	Branjevina	Moderate	SRB_6	10	19.169440	45.467220	80	731.3	14.44	Kostić et al., 2019
		Moderate	SRB_7	10	19.169440	45.467220	80	731.1	14.46	Kostić et al., 2019
		Moderate	SRB_8	10	19.193889	45.520278	80	713.4	12.47	Stojanović et al., 2015b
		Moderate	SRB_9	10	19.193889	45.520278	80	714.4	12.47	Stojanović et al., 2015b
	Smogava	Wet	SRB_10	18	19.211111	44.955833	86	824.6	13.17	Stojanović et al., 2015a
		Wet	SRB_11	12	19.211111	44.955833	86	765.9	14.36	Stojanović et al., 2015a
	Stara vratična	Dry	SRB_12	10	19.245556	44.916111	78	638.5	13.82	Stojanović et al., 2015a
		Dry	SRB_13	13	19.245556	44.916111	78	638.4	13.55	Stojanović et al., 2015a
Bulgaria	Tulovska koriya	Wet	BGR_1	21	25.555320	42.559065	322	757.7	14.47	Unpublished data
	Yulievska koriya	Moderate	BGR_2	20	25.596784	42.565882	311	732.3	14.27	Unpublished data

	Dolna topchiya	Moderate	BGR_3	6	26.556511	42.178805	104	726.4	12.45	Unpublished data
	Gorna topchiya	Dry	BGR_4	18	26.571423	42.261771	124	586.6	12.57	Unpublished data

Note: (*) Timespan: 1950-2018.

Table 2. Generalized additive mixed model (GAMM) outputs to oaks that growing on drier, moderate, and wetter stands.

	DRY			**MODERATE**			**WET**		
Variable	**EDF**	**F (p)**	**k-index (*p*)**	**EDF**	**F (p)**	**k-index**	**EDF**	**F (p)**	**k-index**
PRCP	1	5.053***	0.93***	1	78.097***	0.93***	0.999	12.653***	0.95*
PRCP$_{MAM}$	4.511	5.780***	0.89***	4.536	8.557**	0.89***	1	7.908**	0.92***
PRCP$_{JJA}$a	5.399	0.206^{NS}	0.91***	6.083	5.189***	0.90***	1	1.452^{NS}	0.95**
PRCP$_{Y2}$	2.656	8.881***	0.89***	1	0.264^{NS}	0.91***	1	18.787***	0.97 *
TEMP	3.006	1.875^{NS}	0.90***	5.073	6.400***	0.91***	0.999	4.928*	0.92***
TEMP$_{MAM}$	4.704	3.365**	0.89***	6.762	5.933***	0.91***	1	11.75***	0.93***
TEMP$_{JJA}$	7.184	3.134**	0.89***	1	3.850*	0.89***	1	0.397^{NS}	0.93***
TEMP$_{Y2}$	7.336	6.591***	0.89***	1	13.410***	0.90***	1	0.501^{NS}	0.92***
SM	1	8.565**	0.88***	7.875	4.625***	0.90***	1	8.049**	0.93***
SM$_{Y2}$	3.939	2.161^{NS}	0.87***	8.164	7.795***	0.90***	0.999	17.97***	0.94**
SM$_{MAM}$	5.782	6.762***	0.90***	8.521	7.600***	0.91***	4.834	3.850**	0.89***
SM$_{JJA}$	4.989	5.490***	0.89***	7.04	8.244***	0.90***	1	0.419^{NS}	0.90***
RWL	8.176	8.367***	0.88***	5.696	7.409***	0.88***	1.001	11.315***	0.93***
RWL$_{MAM}$	6.837	7.924***	0.89***	8.316	14.464***	0.89***	1	27.029***	0.93***
RWL$_{JJA}$	8.648	17.069***	0.89***	7.529	6.463***	0.89***	1	10.646**	0.92***
SPI 3$_{MAR}$	4.983	4.380**	0.88***	1	0.459^{NS}	0.90***	0.999	34.684***	0.91***
SPI 3$_{JUN}$	7.633	4.716***	0.88***	7.541	11.657***	0.89***	1.001	28.003***	0.92***
SPI 3$_{AUG}$	6.228	8.016***	0.89***	3.403	4.557*	0.90***	1.001	2.726^{NS}	0.94*
SPI 6$_{MAR}$	1	6.082*	0.89***	1	0.480^{NS}	0.90***	1	17.028***	0.92***
SPI 6$_{JUN}$	0.999	0.893^{NS}	0.89***	4.286	6.305***	0.90***	0.999	36.312***	0.94**
SPI 6$_{AUG}$	0.999	2.965^{NS}	0.91***	5.495	5.779***	0.89***	2.178	2.790^{NS}	0.94***
SPI 12$_{MAR}$	2.600	15.024***	0.90***	1	21.757***	0.91***	1	0.011^{NS}	0.95*
SPI 12$_{JUN}$	1	2.186^{NS}	0.88***	1	48.141***	0.89***	1	0.827^{NS}	0.93***
SPI 12$_{AUG}$	1	0.469^{NS}	0.88***	1	1.905^{NS}	0.92***	0.999	18.575***	0.94**
SPI 24$_{MAR}$	5.198	3.974**	0.89***	1	0.253^{NS}	0.91***	1	29.598***	0.92***
SPI 24$_{JUN}$	7.154	10.926***	0.88***	1.050	0.266^{NS}	0.90***	1	8.244***	0.93***
SPI 24$_{AUG}$	5.562	11.340***	0.89***	6.507	8.732***	0.91***	6.073	6.226***	0.94***
SPI 36$_{MAR}$	1	23.579***	0.87***	4.681	8.743***	0.90***	3.902	5.697***	0.92***
SPI 36$_{JUN}$	5.225	8.050***	0.88***	1	4.433*	0.88***	1	8.194***	0.94**
SPI 36$_{AUG}$	1	1.113^{NS}	0.90***	1.002	3.069^{NS}	0.90***	1	0.186^{NS}	0.91***
SPI 48$_{MAR}$	1	0.023^{NS}	0.88***	1	0.437^{NS}	0.89***	1	0.360^{NS}	0.93***
SPI 48$_{JUN}$	5.133	12.753***	0.87***	7.020	21.690***	0.89***	0.999	0.047^{NS}	0.92***
SPI 48$_{AUG}$	1	33.681***	0.89***	1	11.882***	0.92***	1	0.014^{NS}	0.92***
SPI 60$_{MAR}$	6.808	5.915***	0.88***	4.219	9.040***	0.89***	1	3.042^{NS}	0.93***
SPI 60$_{JUN}$	1	0.648^{NS}	0.88***	1	5.292*	0.90***	1.003	1.295^{NS}	0.92***
SPI 60$_{AUG}$	1	0.054^{NS}	0.90***	1	9.336**	0.90***	3.672	12.421***	0.94***
EQ	5.886	9.366***	0.88***	7.725	21.478***	0.89 ***	2.849	8.072***	0.92***
	Adj R^2=0.570 n=3397		K=9	Adj R^2=0.459 n=4433		K=9	Adj R^2=0.436 n=2201		K=9

Note: **GAMM** - Generalized additive mixed model; **EDF –** Estimated degree of freedom (GAMM); **F –** Fisher test (GAMM); ***p* –** statistically significance. **Signif. code:** (^{ns}) – non-significant; (*) <0.1, (**) <0.01; (***) <0.001. Timespan = 1980 – 2010.

Declaration of interests

☒ The authors declare that they have no known competing financial interests or personal relationships that could have appeared to influence the work reported in this paper.

☒The authors declare the following financial interests/personal relationships which may be considered as potential competing interests:

Title: Different tree-ring width sensitivities to satellite-based soil moisture from dry, moderate and wet pedunculate oak (*Quercus robur* L.) stands across a southeastern distribution margin

Author block: *Saša Kostić, Wolfgang Wagner, Saša Orlović, Tom Levanič, Tzvetan Zlatanov, Ernest Goršić, Lazar Kesić, Bratislav Matović, Nickolay Tsvetanov, Dejan B. Stojanović*

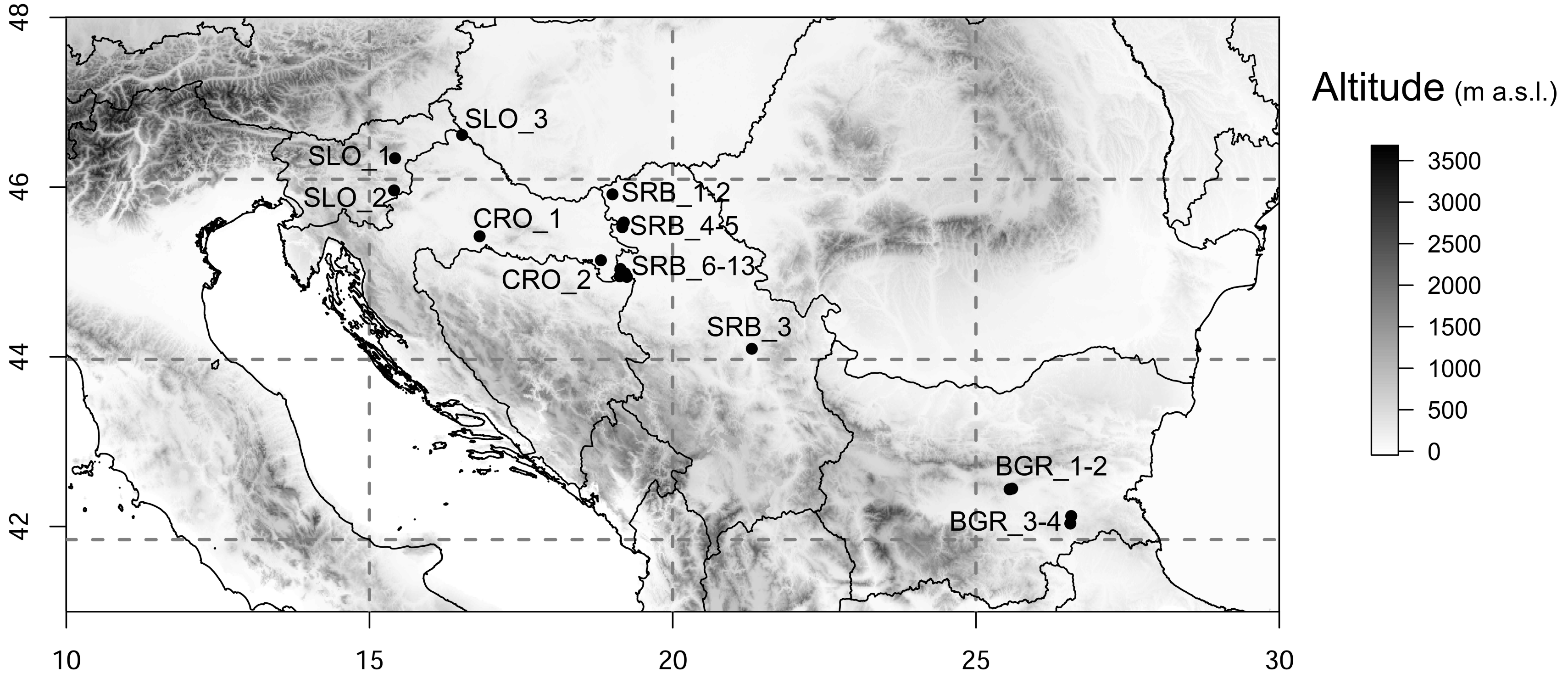

Altitude (m a.s.l.)
3500
3000
2500
2000
1500
1000
500
0
SLO_3
SLO_1
SLO_2
CRO_1
CRO_2
SRB_1-2
SRB_4-5
SRB_6-13
SRB_3
BGR_1-2
BGR_3-4
48
46
44
42
10
15
20
25
30

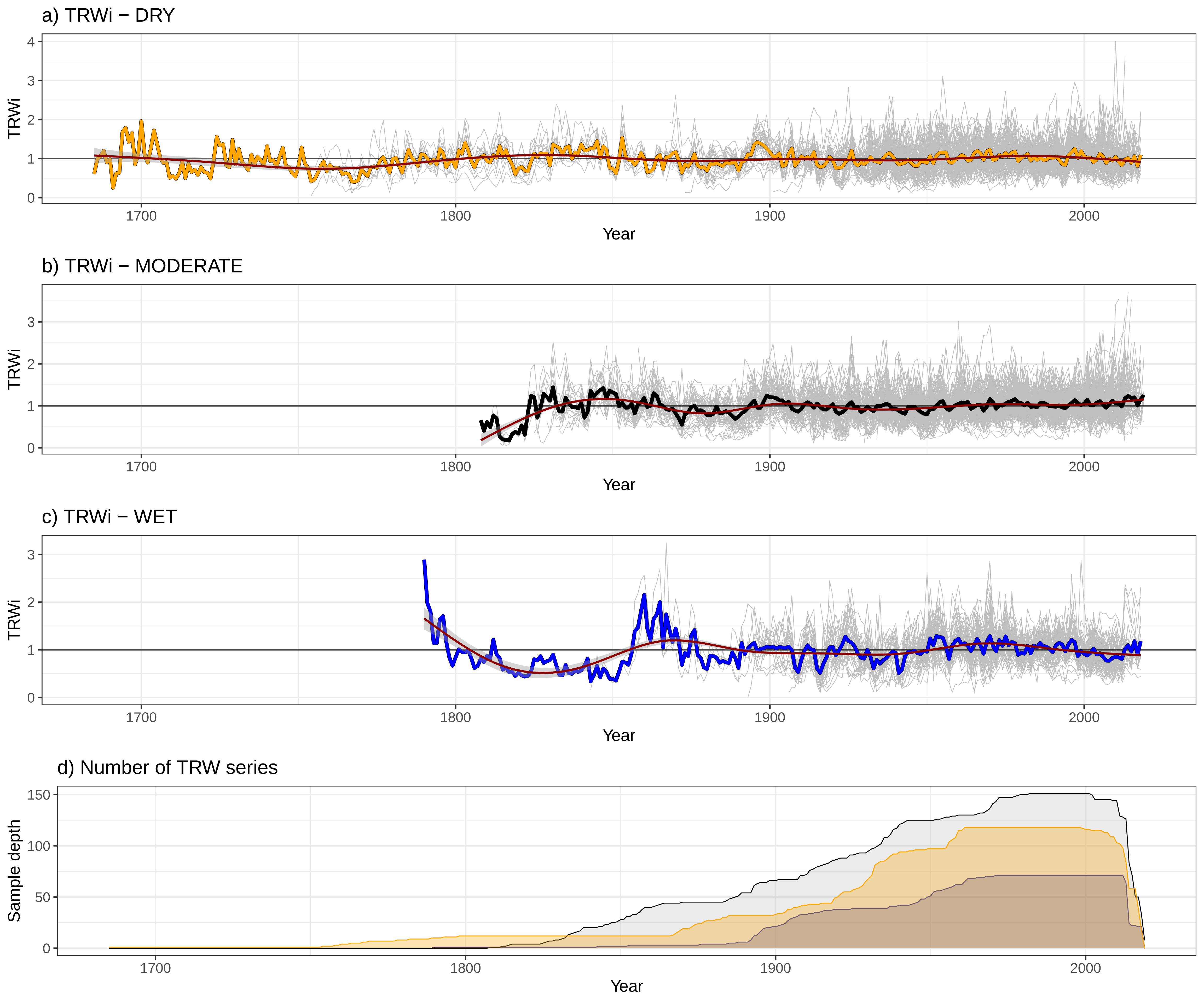

a) TRWi − DRY
TRWi
Year
b) TRWi − MODERATE
TRWi
Year
c) TRWi − WET
TRWi
Year
d) Number of TRW series
Sample depth
Year

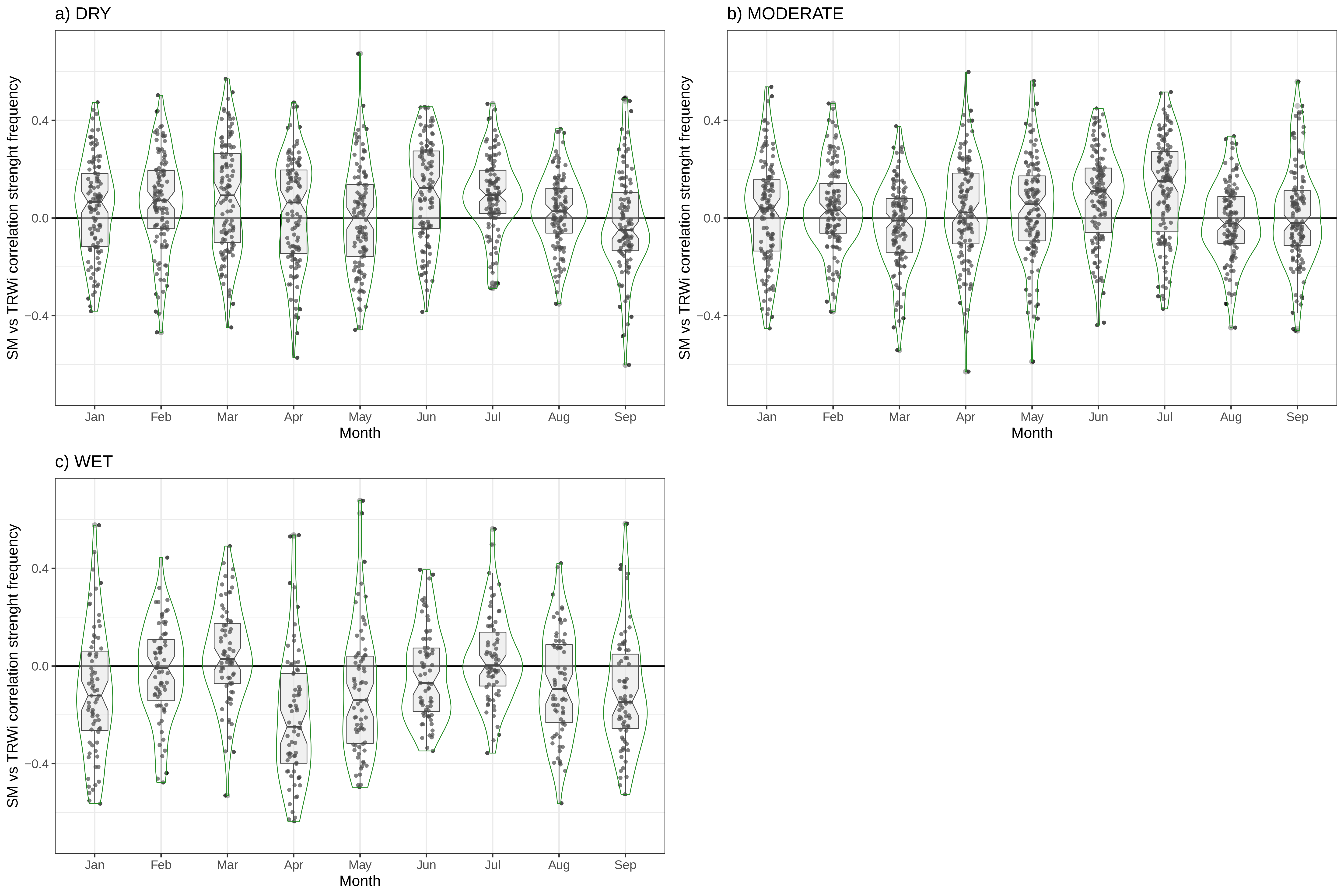
a) DRY
b) MODERATE
c) WET
SM vs TRWi correlation strenght frequency
0.4
0.0
-0.4
Jan
Feb
Mar
Apr
May
Jun
Jul
Aug
Sep
Month

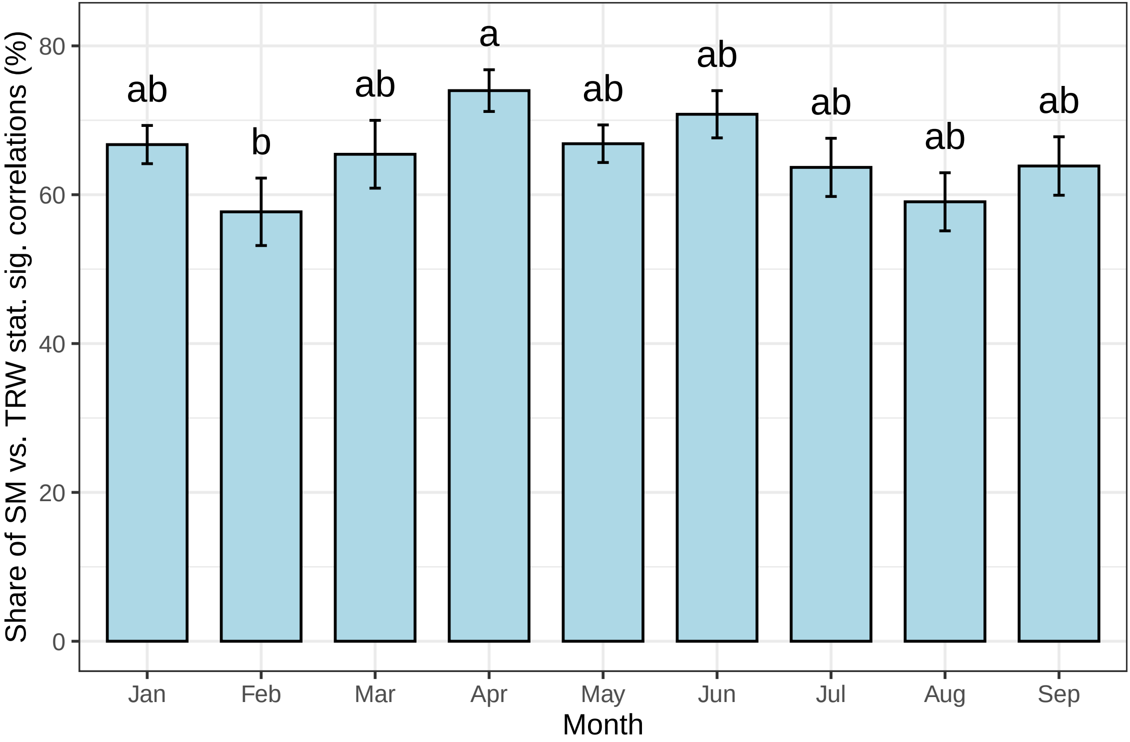

Share of SM vs. TRW stat. sig. correlations (%)
80
60
40
20
0
ab
b
ab
a
ab
ab
ab
ab
ab
Jan
Feb
Mar
Apr
May
Jun
Jul
Aug
Sep
Month

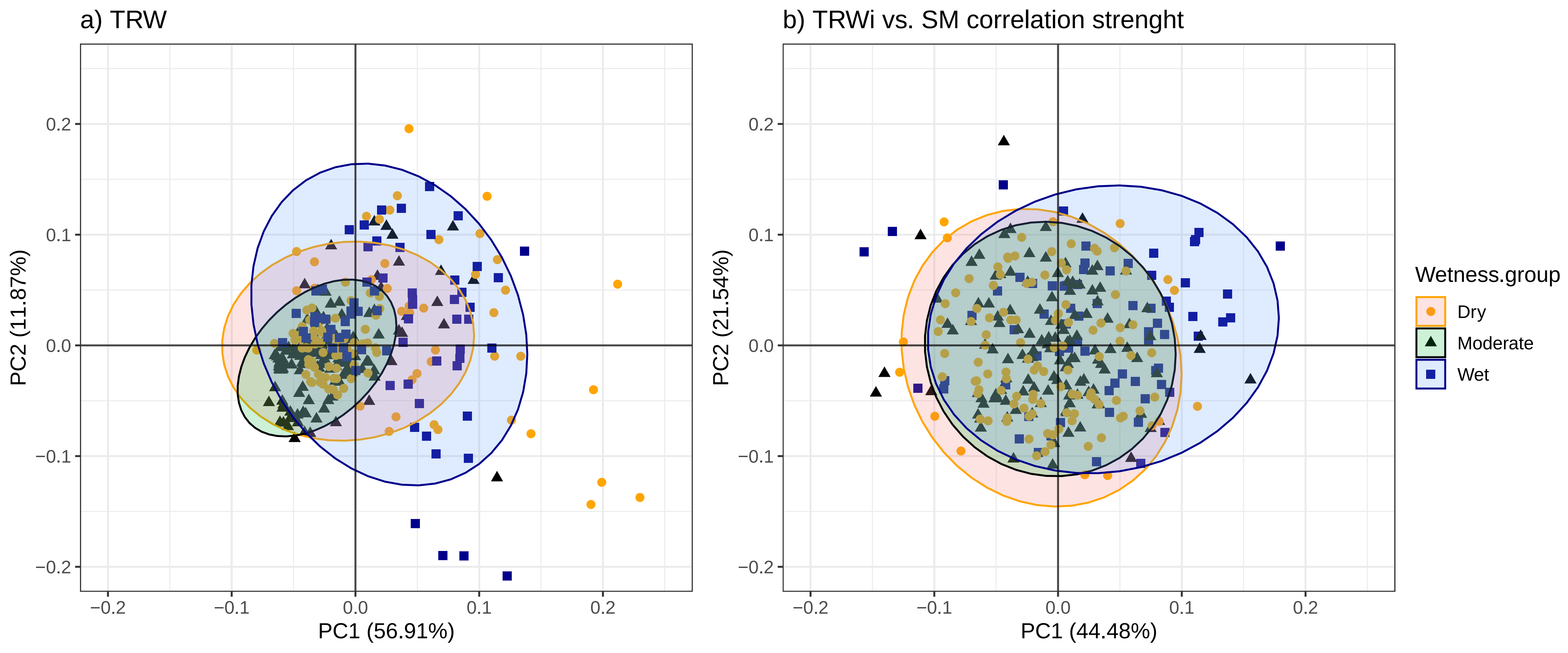

a) TRW
b) TRWi vs. SM correlation strenght
PC1 (56.91%)
PC2 (11.87%)
PC1 (44.48%)
PC2 (21.54%)
−0.2
−0.1
0.0
0.1
0.2
Wetness.group
Dry
Moderate
Wet

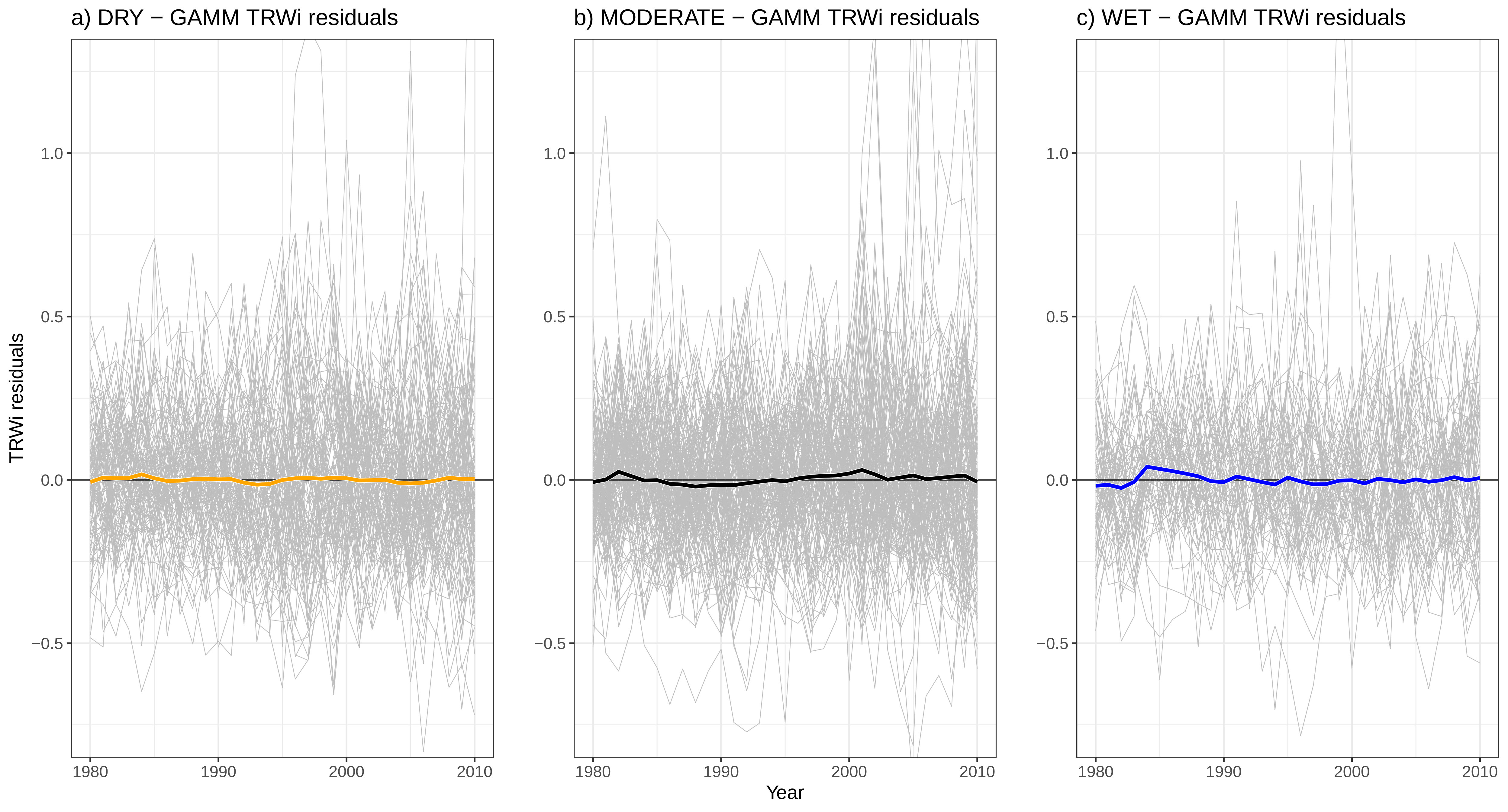
a) DRY − GAMM TRWi residuals
b) MODERATE − GAMM TRWi residuals
c) WET − GAMM TRWi residuals
TRWi residuals
1.0
0.5
0.0
−0.5
1980
1990
2000
2010
Year